

## Research Article

# Microstructure and Properties of TiSiN/AlN with Different Modulation Periods

Hongjuan Yan , Qinye Tian, Fengbin Liu, Lina Si, Zhaoliang Dou, and Shuting Zhang

School of Mechanical and Materials Engineering, North China University of Technology, Beijing, China

Correspondence should be addressed to Hongjuan Yan; [yanhongj@sina.com](mailto:yanhongj@sina.com)

Received 8 May 2019; Accepted 17 September 2019; Published 20 October 2019

Guest Editor: Dinh Gia Ninh

Copyright © 2019 Hongjuan Yan et al. This is an open access article distributed under the Creative Commons Attribution License, which permits unrestricted use, distribution, and reproduction in any medium, provided the original work is properly cited.

TiSiN/AlN nanomultilayers with different thicknesses of AlN layer were deposited on 304 stainless steel by magnetron sputtering system. X-ray diffraction, nanoindentation tester, atomic force microscopy, and friction wear tester were used to characterize microstructure and properties of TiSiN/AlN nanomultilayers. The results show that TiSiN/AlN nanomultilayers are face-centered cubic structures and exhibit a strong preferred orientation on (200) plane. The diffraction peaks of TiSiN/AlN nanomultilayer shift to a small angle. When the thickness of the AlN layer is 2 nm, the peak is highest, and the shift degree is biggest. The alternating tension and compression stress fields are formed along the growth direction of TiSiN/AlN nanomultilayers and increase the strength of the nanomultilayers. When the thickness of the AlN layer is 2 nm, the maximum hardness and Young's modulus of TiSiN/AlN nanomultilayers are, respectively, 32.8 GPa and 472 GPa, and the smallest roughness is 33.4 nm. But the friction coefficient is smallest when the thickness of the AlN layer is 1.5 nm.

## 1. Introduction

The development tendencies of advanced manufacturing technology are high speed, high precision, greening, and intelligent. There is a higher demand for tools in dry cutting. The materials of tool coatings are constantly updated, from binary coating and ternary coating to multilayer coatings [1]. Compared with the monolayer coating, the nanomultilayers deposited alternatively with two or more kinds of materials have higher hardness and good wear resistance. The modulation period (namely bilayer thickness) of nanomultilayers is the thickness of the two adjacent layers. The nanomultilayers are one of the hot points in tool coatings [2–6]. Under the “template effect” of CrAlN layer, SiO<sub>2</sub> grow epitaxially with CrAlN and CrAlN/SiO<sub>2</sub> nanomultilayered films exhibit a face-centered cubic of CrN phase with (200) prefer orientation. When the thickness of SiO<sub>2</sub> layer was 0.7 nm, the maximum values of hardness and Young's modulus reach 38.9 GPa and 425 GPa, respectively [7]. VN layers were inserted periodically in TiAlN layers. The friction coefficient of TiAlN film is about 0.9, while one of TiAlN/VN nanomultilayers can be decreased significantly and reaches a

minimum value of ~0.4 [8]. The TiN/TiAlN nanomultilayer coating is preferentially grown on the (111) crystal plane, and the hardness and Young's modulus are, respectively, 38.9 GPa and 519 GPa at a modulation period of 164 nm [9]. Therefore, many factors such as the composition and the modulation period affect the coating properties. However, research studies on nanomultilayers mainly focus on the synthesis of two single-phase materials. The microstructure and properties of nanomultilayers synthesized with two-phase or multiphase compounds are still unclear. So, it has become a research hotspot of nanomultilayers. TiSiN coatings have a two-phase nc-TiN/Si<sub>3</sub>N<sub>4</sub> structure (amorphous Si<sub>3</sub>N<sub>4</sub> phases surround crystalline TiN phases). A small amount of Si element is added to TiN to prepare a TiSiN nanocomposite, which improves the morphology and hardness of the films [10–14]. The TiVN/TiSiN multilayers have a maximum hardness of 37 GPa, Young's modulus of 315 GPa, and a minimum coefficient of friction of 0.24, which is superior to TiVN and TiSiN films [15]. The NbN/CrSiN nanomultilayers exhibit columnar crystal, and the CrSiN layer is transformed into a face-centered cubic structure under the “template effect” of the NbB layer. When

the Si content is 12%, the hardness and Young's modulus of the NbN/CrSiN nanomultilayers are, respectively, as high as 31.92 GPa and 359.3 GPa [16]. The TiSiN/Ag nanomultilayers contain nc-TiN, nc-Ag crystal phase and Si<sub>3</sub>N<sub>4</sub> amorphous phase with a hardness of 30.56 GPa, and Young's modulus of 513 GPa, which can effectively prevent crack propagation and fracture resistance [17]. Therefore the morphology of TiSiN in TiSiN nanomultilayers is controversial and needs further study.

TiSiN/AlN nanomultilayers with different AlN layer thicknesses were prepared on 304 stainless steel using a vacuum multitarget magnetron sputtering system. X-ray diffractometer, nanoindentation tester, atomic force microscope, and friction-wear tester were used to characterize and analyze microstructure and properties of nanomultilayers. The effects of the thickness of the AlN layer on microstructure and hardness, surface roughness, friction, and wear properties were investigated.

## 2. Experimental Details

**2.1. Materials of Substrates and Targets.** The material of the substrate is 304 stainless steel, the diameter is  $\Phi 20$  mm, and the thickness is 3 mm. The substrates are polished. The substrates are cleaned by the ultrasonic cleaner using ethanol solution.

The targets are the TiSi alloy target and the Al target. The Si content of the TiSi target is 10%, and the purity of Al target is 99.9%. The target size is  $\Phi 50.8$  mm  $\times$  2 mm.

**2.2. Specimens Preparation.** TiSiN/AlN nanomultilayers are deposited on 304 stainless steel substrates using a JCP-350M2 vacuum multitarget magnetron sputtering system. The geometrical arrangement of magnetrons is shown in Figure 1. The substrates are floating, and no bias. The substrate-to-target distance is 80 mm. The vacuum chamber is evacuated to a base pressure of  $3.0 \times 10^{-3}$  Pa. The total operating pressure is maintained at 0.3 Pa, with flow rates of nitrogen, argon of 3 ml/min and 9 ml/min, respectively. The Al target and the TiSi target are, respectively, controlled by a DC and RF power of 110 W and 80 W, and are sputtered for 5 min to remove the oxide layer and impurities of the targets. The substrates are etched with argon for 15 min at bias voltage of  $-700$  V. The thicknesses of TiSiN layer and AlN layer are controlled by the alternate opening and closing of the TiSi target and the Al target shutters. The deposition rates of TiSiN and AlN are about 0.046 nm/s and 0.134 nm/s, respectively. The opening time of the TiSiN target shutters is 21.7 s, and the opening times of the AlN target are 7.5 s, 11.9 s, 14.9 s, 18.65 s, and 22.4 s, respectively. In order to improve the adhesion between the film and the substrate, the TiN layer with 20 nm is deposited as the first layer. Then the AlN layer and the TiSiN layer are alternately deposited. The TiSiN layer is the last layer at coating surface. The total thickness of the nanomultilayers is about 1.2  $\mu$ m. The TiSiN film and the TiSiN/AlN nanomultilayers with different AlN thickness are deposited on 304 stainless steel substrates (shown in Table 1).

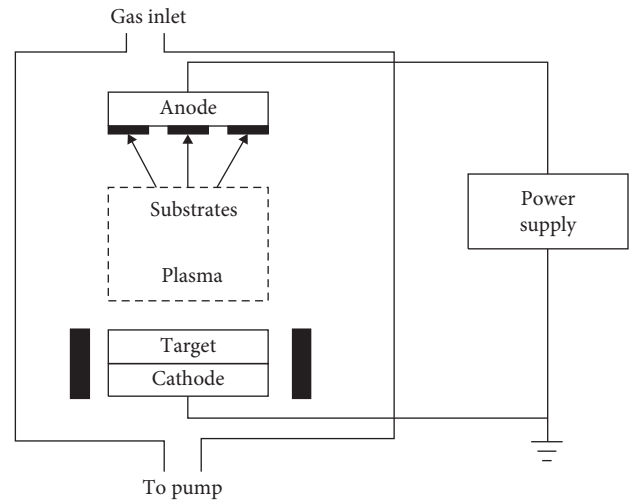


FIGURE 1: Schematic diagram of the magnetron sputtering system.

**2.3. Nanomultilayer Characterization.** The microstructure of TiSiN/AlN nanomultilayers is investigated using a Rigaku X-ray diffractometer with a copper target Cu-K $\alpha$ . The wavelength of Cu-K $\alpha$  is 1.5406 Å, the current is 40 mA, the voltage is 40 kV, the scanning speed is 8° (s), the scanning step size is 0.02°, and the scanning range is 10°~80°. The hardness and Young's modulus of TiSiN/AlN nanomultilayers are measured using a nanoindentation tester, with the load of 10 mN, the loading rate of 20 mN/min, the approach speed of 1000 nm/min, and the load holding time of 5 s. The roughness of the nanomultilayers is observed using a CSPM-5500 atomic force microscope of Guangzhou Prima Technology Co., Ltd. The scanning method is contact scanning, the scanning frequency is 2 Hz, and the scanning range is 2000 nm  $\times$  2000 nm. The tribological performance is evaluated by CFT-I material surface performance tester of Lanzhou Zhongke Kaihua Technology Development Co., Ltd. The 6 mm-diameter GCr15 ball is the counter material. The experimental load is 80 g. The linear speed is 40 mm/s, and the running length is 5 mm. The test time is 5 min. The electronic balance with an accuracy of 0.0001 g used to measure the quality of the specimens before and after wear test.

## 3. Results and Discussion

**3.1. Structure.** Figure 2 shows the XRD patterns of TiSiN film and TiSiN/AlN nanomultilayers with different AlN layer thicknesses. The structure of TiSiN/AlN nanomultilayers with different modulation periods is significantly different. TiSiN/AlN nanomultilayers exhibit NaCl face-centered cubic structures with no obvious orientation on the (111) crystal plane and exhibit preferential orientation on the (200) crystal plane because the nanomultilayers are sputtered at low values of energy  $E_{bi}$  controlled by the substrate bias [18]. The peaks of TiSiN/AlN nanomultilayers shift to a small degree in Figure 2. When the thickness of AlN layer is 2 nm, the intensity of the diffraction peak corresponding to the nanomultilayers is the highest, and the largest shift angle

TABLE 1: Modulation periods of TiSiN/AlN nanomultilayers.

No.	$t_{\text{TiSiN}}$ (s)	$t_{\text{AlN}}$ (s)	$l_{\text{TiSiN}}$ (nm)	$l_{\text{AlN}}$ (nm)	Modulation period (nm)	Number of bilayers	Total thickness ( $\mu\text{m}$ )
1	21.7	7.5	1	1	2	600	1.2
2	21.7	11.19	1	1.5	2.5	500	1.25
3	21.7	14.9	1	2	3	400	1.2
4	21.7	18.65	1	2.5	3.5	350	1.225
5	21.7	22.4	1	3	4	300	1.2

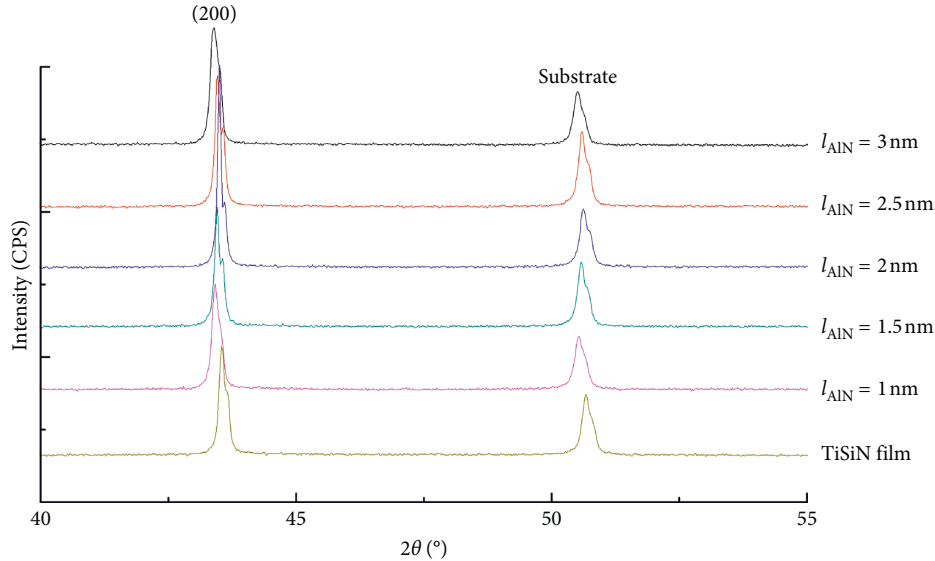


FIGURE 2: XRD patterns of TiSiN/AlN nanomultilayers and monolithic TiSiN film.

is  $0.14^\circ$ . According to the Bragg's equation [19–21], the interplanar spacings increase from 0.2236 nm to 0.2242 nm.

Many researches were conducted on CrAlN/SiO<sub>2</sub> [6], VN/TiB<sub>2</sub> [22], ZrN/SiN<sub>x</sub> [23], TiAlN/AlN [24], TiSiN/TiN [25], TiSiN/CrAlN [26], and TiAlN/TiN [27]. The results showed that coherent growth occurs between the two layers of the nanomultilayers. In Figure 2, when the thickness of the AlN layer is less than 2 nm, the AlN layer and TiSiN layer grow epitaxial, which promotes the growth of TiSiN/AlN nanomultilayer structure on the (200) crystal plane, so the diffraction peak of the XRD spectrum increase. However, when the thickness of AlN layer is thicker than 2 nm, the coherent growth structure is broken. The microstructure of TiSiN/AlN nanomultilayers alternately grows as “brick wall” modulation structure [28], so the diffraction peak lower in Figure 2.

The lattice constant of AlN is 0.2491 nm and bigger than the one of TiSiN. When the AlN layer and TiSiN layer grow epitaxial, AlN layer transforms to a face-centered cubic structure under the template effect of the TiSiN layer [22–27]. The lattice constant of the TiSiN layer increases and the one of AlN layer decreases at the interface. So the lattice constant of TiSiN/AlN nanomultilayers is bigger than TiSiN film, which causes the degree of diffraction peak to shift to a small angle.

**3.2. Hardness and Young's Modulus.** Figure 3 shows the relationship between hardness and Young's modulus of TiSiN/AlN nanomultilayers versus the thickness of the AlN

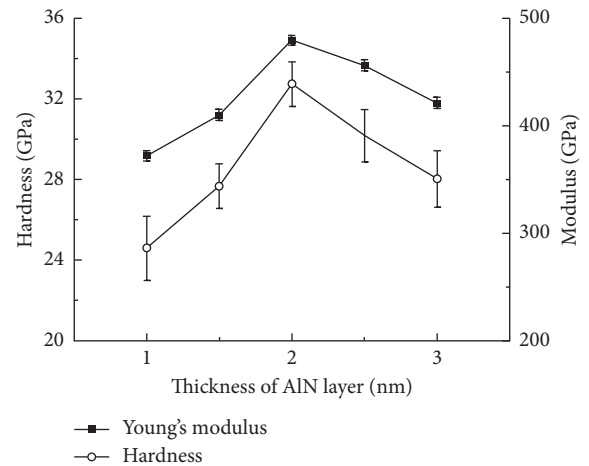


FIGURE 3: Hardness and Young's modulus of TiSiN/AlN nanomultilayers with different thicknesses of AlN layer.

layer. The hardness and Young's modulus of TiSiN/AlN nanomultilayers firstly increases and then decreases with the thickness of the AlN layer. When the thickness of the AlN layer is less than 2 nm, the hardness and Young's modulus of TiSiN/AlN nanomultilayers increase with the thickness of the AlN layer. When the thickness of the AlN layer is 2 nm, the hardness and Young's modulus of TiSiN/AlN nanomultilayers reach a maximum value of  $32.8 \text{ GPa} \pm 1.1 \text{ GPa}$  and  $47.2 \text{ GPa} \pm 4.8 \text{ GPa}$ , respectively, and  $H/E$  is about 0.07.

When the thickness of the AlN layer is larger than 2 nm, the hardness and Young's modulus of TiSiN/AlN nanomultilayers decrease with the thickness of the AlN layer.

The interfacial strengthening of nanomultilayers has different strengthening mechanisms such as Koehler models [29], Hall–Petch effect [30], and alternating stress field effect [31]. In Koehler models, dislocations have different line energy densities when the two modulation layers have different elastic moduli. During the deposition of TiSiN/AlN nanomultilayers, the dislocations pass through the interface between TiSiN layer and AlN layer and are hindered by the mirror force applied to the interface of the multilayers which causes the strengthening of the nanomultilayers. However, when the thickness of the AlN layer exceeds a certain range, the interface will hinder the dislocation motion, make it unable to penetrate AlN layer growth. It will destroy the epitaxial growth of TiSiN layer and AlN layer. Then the hardness reduces [7].

The change in the thickness of the AlN layer has effects on the growth of the AlN columnar crystal along the growth direction of TiSiN/AlN nanomultilayers [32]. Therefore, when AlN layer and TiSiN layer are alternately deposited, the difference in the lattice constant of the two layers causes stress at the interface. AlN is a close-packed hexagonal structure with a larger lattice constant, so there is a compressive stress in AlN layer. The lattice constant of TiSiN layer is relatively small, so there is tensile stress. Therefore, the tensile and compressive alternate stress field with a modulation period is formed along the growth direction of nanomultilayers. When the thickness of the AlN layer is 2 nm, the diffraction peak of TiSiN/AlN nanomultilayers on the XRD pattern is shifted to a small degree, and the alternative stress at the interface between TiSiN layer and AlN layer is the largest. According to alternating stress field effect, nanomultilayers that are comprised of two different lattice constant materials have a lattice mismatch in the two modulation layers. The lattice distortion occurs at the interface. The tensile and compressive stress field has a hard effect on the nanomultilayers [24].

**3.3. Roughness.** Figure 4 shows the relationship between the surface roughness of TiSiN/AlN nanomultilayers and the thickness of the AlN layer. With the thickness of the AlN layer, the surface roughness of TiSiN/AlN nanomultilayers decreases first and then increases. When the thickness of the AlN layer is 2 nm, the surface roughness of TiSiN/AlN nanomultilayers is 33.4 nm, and the surface is the smoothest. The roughness of TiSiN/AlN nanomultilayers with 3-nm thick AlN layers is biggest because the surface roughness of TiSiN/AlN nanomultilayers is closely related to the nucleation process. When the thickness of the AlN layer is 3 nm, the AlN layer has a long deposition time and a large grain size.

**3.4. Tribological Properties.** Figure 5 shows the relationship between the tribological properties of TiSiN film and TiSiN/AlN nanomultilayers and the thickness of the AlN layer. The friction coefficient of TiSiN film is bigger than the ones of TiSiN/AlN nanomultilayers. With the thickness of the AlN

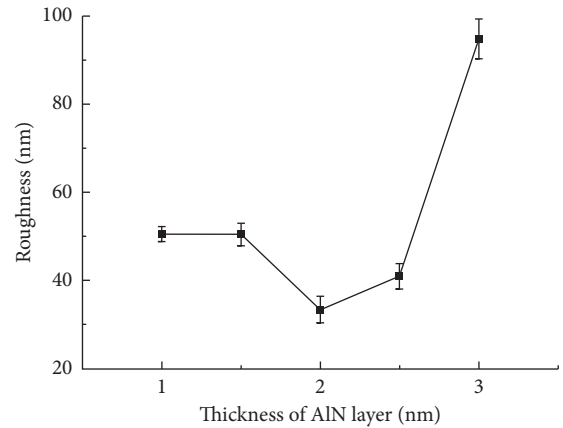


FIGURE 4: Surface roughness of TiSiN/AlN nanomultilayers with different thicknesses of AlN layer.

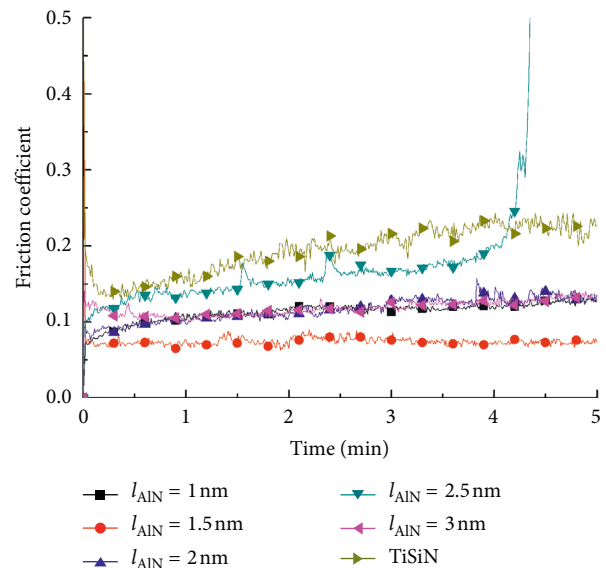


FIGURE 5: Friction coefficient of TiSiN/AlN nanomultilayers with different thicknesses of AlN layer and monolithic TiSiN film.

layer, the friction coefficient of TiSiN/AlN nanomultilayers decreases firstly and then increases. When the thickness of the AlN layer is 1.5 nm, the friction coefficient is the smallest and very stable. When the thickness of the AlN layer is 2.5 nm, the friction coefficient is the largest, and it increases rapidly when the experimental time is more than 4 min. The reason is that the film breaks and falls off the substrate. When the thickness of the AlN layer is 1 nm, 2 nm, and 3 nm, the friction coefficients are similar.

Figure 6 shows the relationship between the abrasion loss of TiSiN/AlN nanomultilayers and the thickness of AlN layer. With the thickness of the AlN layer, the abrasion loss of TiSiN/AlN nanomultilayers decreases firstly and then increases. When the thickness of AlN layer is 1.5 nm, the abrasion loss is the smallest. The results are consistent with the friction coefficients of TiSiN/AlN nanomultilayers.

Figure 7 shows the wear track morphology was observed under an optical microscope after the friction and wear test

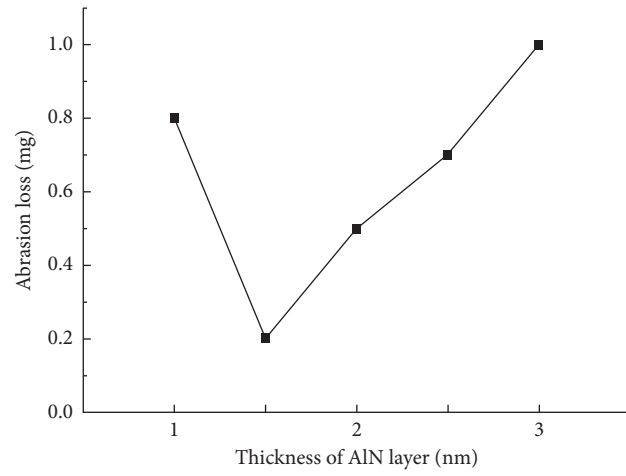


FIGURE 6: Abrasion loss of TiSiN/AlN nanomultilayers with different thicknesses of AlN layer.

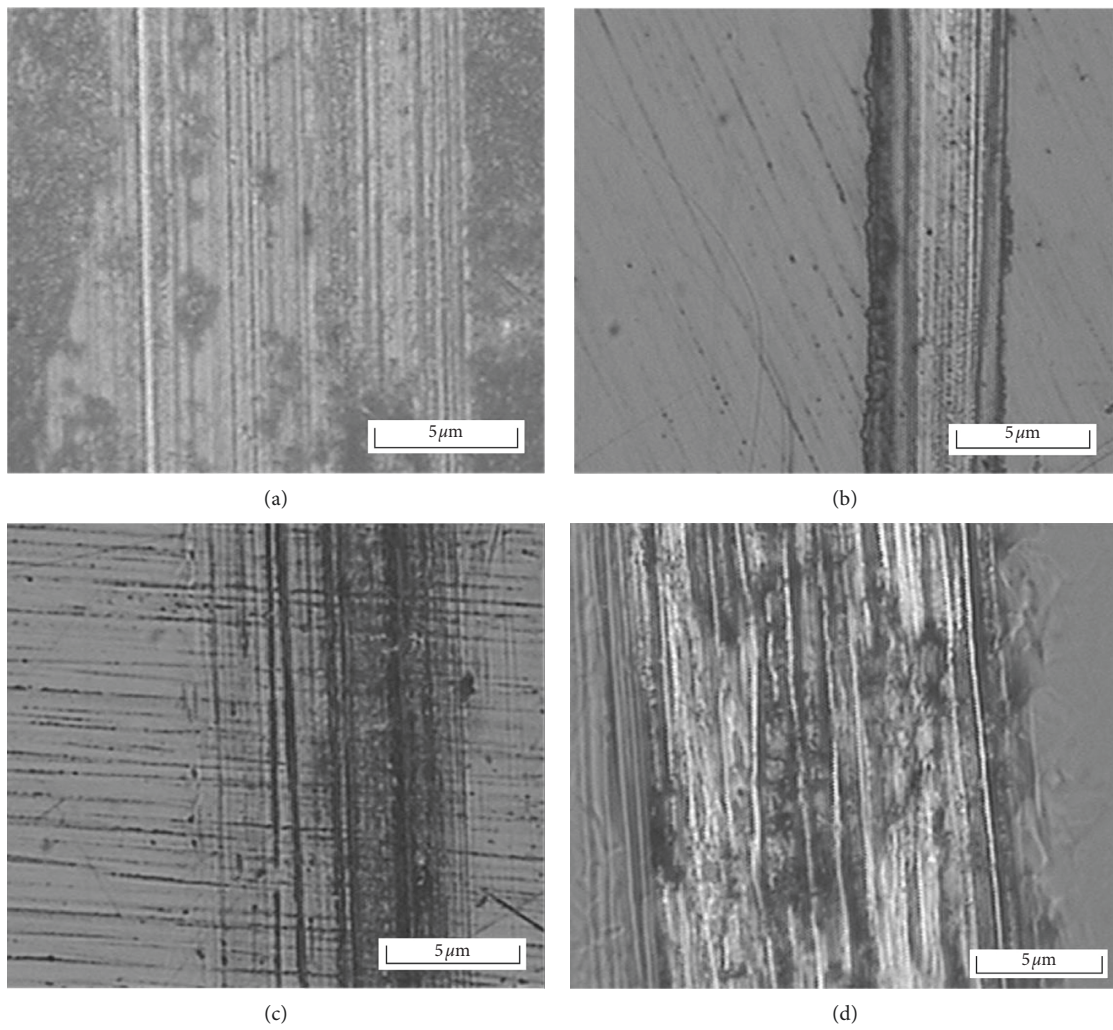
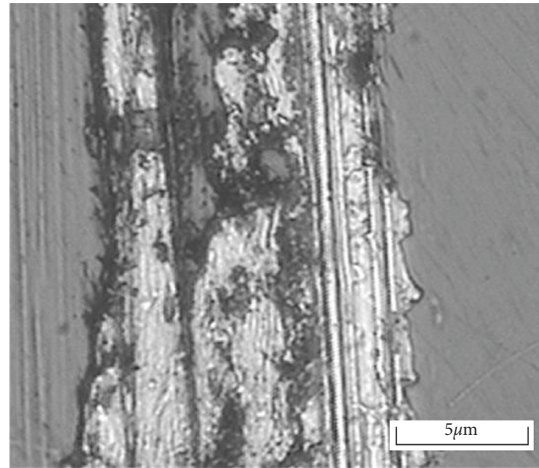


FIGURE 7: Continued.



(e)

FIGURE 7: Morphology of TiSiN/AlN nanomultilayers. (a) Thickness of the AlN layer is 1 nm. (b) Thickness of the AlN layer is 1.5 nm. (c) Thickness of the AlN layer is 2 nm. (d) Thickness of the AlN layer is 2.5 nm. (e) Thickness of the AlN layer is 3 nm.

of TiSiN/AlN nanomultilayers. When the thickness of the AlN layer is 1 nm, 1.5 nm, and 2 nm, the surfaces of nanomultilayers have furrows with different depth and obvious plastic deformation. The wear mechanism is abrasive wear. When the thickness of AlN layer is 1.5 nm, the wear tracks are relatively shallow and narrow, which is consistent with the small and stable friction coefficient in Figure 5. When the thickness of the AlN layer is 2.5 nm and 3 nm, the nanomultilayers wear sharply. The surfaces have deeper furrows and severe adhesive wear. Especially when the thickness of AlN layer is 2.5 nm, wrinkles appear on the right edge of wear track which indicates that the nanomultilayers are worn through. Because the nanomultilayers have higher hardness, the contact stress causes the nanomultilayers peeling from the substrate. So the friction coefficient suddenly increases when the wear time is more than 4 min in Figure 5. When the thickness of the AlN layer is 3 nm, the initial wear friction coefficient is larger because the surface roughness is largest. The friction force is relatively bigger, so the wear track shows severe abrasive wear and adhesive wear.

#### 4. Conclusion

- (1) The TiSiN/AlN nanomultilayers with different thicknesses of the AlN layer were deposited on 304 stainless steel using magnetron sputtering. The effect of modulation period on the properties of TiSiN/AlN nanomultilayers was investigated.
- (2) The TiSiN/AlN nanomultilayers are all face-centered cubic structures with a preferential orientation at the (200) plane, and the diffraction peaks shifted to small angles. When the thickness of the AlN layer is less than 2 nm, the AlN layer and TiSiN layer exhibit epitaxial growth, and the TiSiN layer and AlN layer form a periodic tensile and compressive alternating stress field, which causes film strengthening.

- (3) With the increase of the thickness of the AlN layer, the hardness and Young's modulus of TiSiN/AlN nanomultilayers increase firstly and then decrease, and the surface roughness, the abrasion loss and friction coefficient decrease firstly and then increase. When the thickness of the AlN layer is 2 nm, the hardness and Young's modulus of TiSiN/AlN nanomultilayers reach, respectively, the maximum of  $32.8 \text{ GPa} \pm 1.1 \text{ GPa}$  and  $472 \text{ GPa} \pm 4.8 \text{ GPa}$ ,  $H/E$  is about 0.07, and the surface roughness is a minimum of 33.4 nm. When the thickness of the AlN layer is 1.5 nm, the wear tracks appear narrow, the friction coefficient is the smallest, and the wear mechanism is mainly abrasive wear.

#### Data Availability

The data of Figure 3 (hardness and Young's modulus of TiSiN/AlN nanomultilayers with different thicknesses of AlN layer) and Figure 4 (surface roughness of TiSiN/AlN nanomultilayers with different thicknesses of AlN layer) used to support the findings of this study are included within the article. The other data of Figure 2 (XRD patterns of TiSiN/AlN nanomultilayers and monolithic TiSiN film) and Figure 5 (Friction coefficient of TiSiN/AlN nanomultilayers with different thicknesses of AlN layer and monolithic TiSiN film) used to support the findings of this study are available from the corresponding author upon request.

#### Conflicts of Interest

The authors declare that there are no conflicts of interest regarding the publication of this paper.

#### Acknowledgments

This work was supported by the National Natural Science Foundation of China (Grant Nos. 51575004, 51775044

and 11704008), Beijing Municipal Science & Technology Commission (No. KZ201910009010), and the Support Plan of Yuyou Youth, Yuyou Innovation Team and Science and Technology Activities of Student from North China University of Technology.

## References

- [1] Q. Zhang, L. Zhao, M. Liu et al., "Research status and development trends of cutting tool coating technology," *Non-ferrous Metals Science and Engineering*, vol. 5, no. 2, pp. 20–25, 2014.
- [2] M. Shinn and S. A. Barnett, "Effect of superlattice layer elastic moduli on hardness," *Applied Physics Letters*, vol. 64, no. 1, pp. 61–63, 1994.
- [3] P. B. Mirkarimi, L. Hultman, and S. A. Barnett, "Enhanced hardness in lattice-matched single-crystal TiN/V<sub>0.6</sub>Nb<sub>0.4</sub>N superlattices," *Applied Physics Letters*, vol. 57, no. 25, pp. 2654–2656, 1990.
- [4] G. Abadias, A. Michel, C. Tromas, C. Jaouen, and S. N. Dub, "Stress, interfacial effects and mechanical properties of nanoscale multilayered coatings," *Surface and Coatings Technology*, vol. 202, no. 4–7, pp. 844–853, 2007.
- [5] X. Sui, G. Li, C. Jiang et al., "Improved toughness of layered architecture TiAlN/CrN coatings for titanium high speed cutting," *Ceramics International*, vol. 44, no. 5, pp. 5629–5635, 2018.
- [6] J. Musil, "Hard nanocomposite coatings: thermal stability, oxidation resistance and toughness," *Surface and Coatings Technology*, vol. 207, pp. 50–65, 2012.
- [7] W. Li, K. Zheng, P. Liu et al., "Microstructure and superhardness effect of CrAlN/SiO<sub>2</sub> nanomultilayered film synthesized by reactive magnetron sputtering," *Materials Characterization*, vol. 118, pp. 79–84, 2016.
- [8] M. Li, E. Wang, J. Yue, and X. Z. Huang, "Microstructure, mechanical and tribological property of TiAlN/VN nanomultilayer films," *Journal of Inorganic Materials*, vol. 32, no. 12, pp. 1820–1824, 2017.
- [9] Y. Wei, X. Zong, Z. Jiang, and X. Tian, "Characterization and mechanical properties of TiN/TiAlN multilayer coatings with different modulation periods," *The International Journal of Advanced Manufacturing Technology*, vol. 96, no. 5–8, pp. 1677–1683, 2017.
- [10] M. Chen, F. Cai, W. Chen, Q. Wang, and S. Zhang, "Influence of vacuum annealing on structures and properties of Al-Ti-Si-N coatings with corrosion resistance," *Surface and Coatings Technology*, vol. 312, pp. 25–31, 2017.
- [11] T. Chengjian and K. Dejun, "Effects of wear speeds on friction-wear behaviours of cathode arc ion plated TiAlSiN coatings at high temperatures," *Tribology—Materials, Surfaces & Interfaces*, vol. 11, no. 2, pp. 66–74, 2017.
- [12] S. Guha, A. Bandyopadhyay, S. Das, and B. Prasad Swain, "Synthesis and characterization of titanium silicon nitride (TiSiN) thin film: a review," *IOP Conference Series: Materials Science and Engineering*, vol. 377, Article ID 012181, 2018.
- [13] L. Shizhi, S. Yulong, and P. Hongrui, "Ti-Si-N films prepared by plasma-enhanced chemical vapor deposition," *Plasma Chemistry and Plasma Processing*, vol. 12, no. 3, pp. 287–297, 1992.
- [14] J. Musil, "Flexible hard nanocomposite coatings," *RSC Advances*, vol. 5, no. 74, pp. 60482–60495, 2015.
- [15] Y.-Y. Chang, H. Chang, L.-J. Jhao, and C.-C. Chuang, "Tribological and mechanical properties of multilayered TiVN/TiSiN coatings synthesized by cathodic arc evaporation," *Surface & Coating Technology*, vol. 350, pp. 1071–1079, 2018.
- [16] Q. Yuan, W. Li, P. Liu et al., "Influence of Si content on microstructure and mechanical property of CrN/TiSiN nanomultilayered films," *Journal of Functional Materials*, vol. 49, no. 1, pp. 1044–1048, 2018.
- [17] C. Dang, Y. Yao, T. Olugbade, J. Li, and L. Wang, "Effect of multi-interfacial structure on fracture resistance of composite TiSiN/Ag/TiSiN multilayer coating," *Thin Solid Films*, vol. 653, pp. 107–112, 2018.
- [18] M. Jaroš, J. Musil, R. Čerstvý, and S. Haviar, "Effect of energy on structure, microstructure and mechanical properties of hard Ti(Al,V)N<sub>x</sub> films prepared by magnetron sputtering," *Surface & Coating Technology*, vol. 332, pp. 190–197, 2017.
- [19] H. Yan, F. Liu, X. Li, and F. Yang, "Research on microstructure and properties of TiAlN/AlON nanomultilayers," *Transactions of Beijing Institute of Technology*, vol. 38, no. 12, pp. 1296–1301, 2018.
- [20] G. Li, Y. Li, and G. Li, "Crystallization of amorphous AlN and superhardness effect in VC/AlN nanomultilayers," *Thin Solid Films*, vol. 520, no. 6, pp. 2032–2035, 2012.
- [21] H. Caliskan, C. C. Celil, and P. Panjan, "Effect of multilayer nanocomposite TiAlSiN/TiSiN/TiAlN coating on wear behavior of carbide tools in the milling of hardened AISI D2 steel," *Journal of Nano Research*, vol. 38, pp. 9–17, 2016.
- [22] Y. Pan, L. Dong, N. Liu, J. Yu, C. Li, and D. Li, "Investigating the influence of epitaxial modulation on the evolution of superhardness of the VN/TiB<sub>2</sub> multilayers," *Applied Surface Science*, vol. 390, pp. 406–411, 2016.
- [23] G. Abadias, V. V. Uglov, I. A. Saladukhin et al., "Growth, structural and mechanical properties of magnetron-sputtered ZrN/SiN<sub>x</sub> nanolaminated coatings," *Surface and Coatings Technology*, vol. 308, pp. 158–167, 2016.
- [24] H. Yan, Q. Tian, D. Gao, and F. Yang, "Microstructure and properties of TiAlN/AlN multilayers with different modulation periods," *Surface and Coatings Technology*, vol. 363, pp. 61–65, 2019.
- [25] Y. X. Xu, L. Chen, Z. Q. Liu, F. Pei, and Y. Du, "Improving thermal stability of TiSiN nanocomposite coatings by multilayered epitaxial growth," *Surface and Coatings Technology*, vol. 321, no. 15, pp. 180–185, 2017.
- [26] W. Li, P. Liu, J. Meng et al., "Microstructure and mechanical property of TiSiN nanocomposite film with inserted CrAlN nanomultilayers," *Surface and Coatings Technology*, vol. 286, pp. 313–318, 2016.
- [27] C. Hu, X. Dong, M. Li et al., "Microstructures and mechanical properties of TiAlN/TiN nano-multilayered films," *Chinese Journal of Vacuum Science and Technology*, vol. 36, no. 7, pp. 807–812, 2016.
- [28] J. Wang, P. Liu, L. Yang et al., "Research on microstructure and mechanical properties of TiAlN/AlON nanomultilayers," *Journal of Mechanical Engineering*, vol. 48, no. 4, pp. 72–77, 2012.
- [29] J. S. Koehler, "Attempt to design a strong solid," *Physical Review B*, vol. 2, no. 2, pp. 547–551, 1970.
- [30] P. M. Anderson and C. Li, "Hall-Petch relations for multilayered materials," *Nanostructured Materials*, vol. 5, no. 3, pp. 349–362, 1995.
- [31] M. Kato, T. Mori, and L. H. Schwartz, "Hardening by spinodal modulated structure," *Acta Metallurgica*, vol. 28, no. 3, pp. 285–290, 1980.
- [32] L. Chen, Y. X. Xu, Y. Du, and Y. Liu, "Effect of bilayer period on structure, mechanical and thermal properties of TiAlN/AlTiN multilayer coatings," *Thin Solid Films*, vol. 592, pp. 207–214, 2015.

